Opportunistic Spectrum Allocation for Max-Min Rate in NC-OFDMA

Ratnesh Kumbhkar, Tejashri Kuber, Gokul Sridharan, Narayan B. Mandayam, Ivan Seskar
WINLAB, Rutgers University
671 Route 1, North Brunswick, NJ, 08902.
Email: {ratnesh, tkuber, gokul, narayan, seskar}@winlab.rutgers.edu

***Abstract*—We envision a scenario for opportunistic spectrum access among multiple point-to-point links when the available spectrum is not contiguous due to the presence of external interference sources. Non-contiguous Orthogonal Frequency Division Multiplexing (NC-OFDM) is a promising technique to utilize such disjoint frequency bands in an efficient manner. In this paper we study the problem of fair spectrum allocation across multiple NC-OFDM-enabled, point-to-point cognitive radio links under certain practical considerations that arise from such non-contiguous access. When using NC-OFDMA, the channels allocated to a cognitive link are spread across several disjoint frequency bands leading to a large *spectrum span* for that link. Increased spectrum span requires higher sampling rates, leading to increased power consumption in the ADC/DAC of the transmit/receive nodes. In this context, this paper proposes a framework for spectrum allocation that maximizes the minimum rate achieved by the cognitive radio links, under a constraint on the maximum permissible spectrum span. Under constant transmit powers and orthogonal spectrum allocation, such an optimization is an integer linear program and can be solved efficiently. There exists a clear trade-off between the max-min rate achieved and the maximum permissible spectrum span. The spectrum allocation obtained from the proposed optimization framework is shown to be close to the trade-off boundary, thus showing the effectiveness of the proposed technique. We find that it is possible to limit the spectrum span without incurring a significant penalty on the max-min rate under different interference environments. We also discuss an experimental evaluation of the techniques developed here using the ORBIT radio network testbed that consists of multiple Universal Software Radio Peripherals (USRPs).**

I. Introduction

With the increasing number of wireless devices, availability of usable spectrum for these devices is a concern. Cognitive radio (CR) plays an important role in addressing this problem with dynamic spectrum access. Over the last few years significant research has been carried out in addressing different aspects of cognitive radios [1]–[10]. Orthogonal frequency division multiplexing (OFDM) has been suggested as one of the candidates for dynamic spectrum access in CRs due to its flexible and efficient use of the spectrum [11]. Non-contiguous OFDM (NC-OFDM) is a method of transmission where some of the subcarriers in OFDM are nulled and only the remaining subcarriers are used for transmission [12]–[14]. Since available unused spectrum is generally non-contiguous, using NC-OFDM results in better spectrum utilization. Further, NC-OFDM allows the CRs to access the unused spectrum without interfering with the licensed users. Techniques for efficient implementation of the DFT operation for NC-OFDM when multiple subcarriers are nulled are also available [12]. However, one main drawback of NC-OFDM is that it suffers from high out-of-band radiation due to the high sidelobes of its modulated subcarriers, which can potentially affect the performance of licensed users, or other CRs in the unlicensed band. Several techniques to address this issue have been proposed and we briefly touch upon these issues in the later part of this paper.

Another significant concern when using NC-OFDMA is that the cognitive links are allocated disjoint frequency bands that lead to an increased spectrum span of a cognitive link. The spectrum span is defined as the difference between the frequencies of the extreme channels allocated to a cognitive link. Increase in the spectrum span leads to higher sampling rates that in turn lead to an increase in the power consumption at the transmit/receive nodes. Traditionally, the transmit power requirements of a transceiver system have dominated the total power consumption. However, the ADC/DAC power consumption can become comparable or even significantly larger than the transmit power consumption when the sampling rates become very large [15]. It is therefore important to impose a reasonable limit on the spectrum span.

In this paper, we consider the problem of spectrum allocation across multiple point-to-point cognitive links between NC-OFDM-enabled transceivers in the presence of interference from out-of-network users. The main goal is to achieve a fair spectrum allocation that maximizes the minimum data rate across these cognitive links while limiting the spectrum span. Towards this goal, we propose an optimization framework to maximize the minimum rate, subject to the constraint that spectrum span does not exceed a certain limit. Under constant transmit powers and orthogonal spectrum allocation, such an optimization is an integer linear program and can be solved efficiently using readily available solvers. Simulation results show a trade-off between the max-min rate and spectrum span. In our simulations, we also show improvement in data rate based on spectrum allocation obtained from solving the optimization problem in presence of interference. We also implement the NC-OFDM system using USRP [16] radios with GNU Radio software platform on ORBIT testbed [17]. GNU Radio is a free and open-source software development toolkit that provides signal processing blocks to implement software radios [18].

The remainder of this paper is organized as follows. In Section II we briefly discuss the existing literature on spectrum allocation and in Section III we present our system model with various channel constraints and allocation constraints with the problem formulation. In Section IV we present our simulation

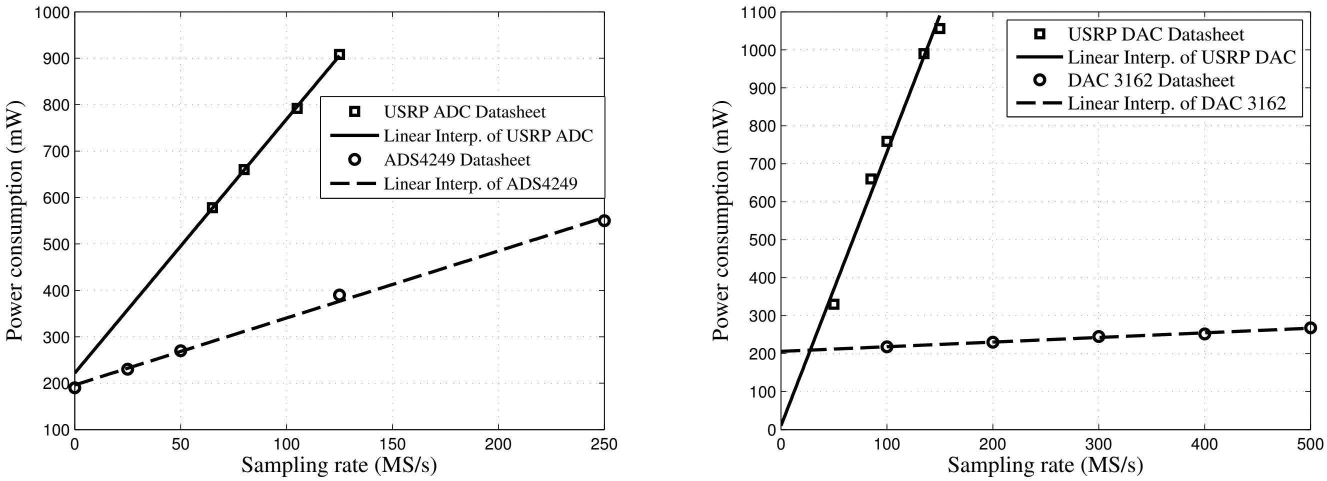

(a) ADS62P4x [19] (ADC of USRP radio) and ADS4249 [20]

(b) AD 9777 [21] (DAC of USRP radio) and DAC 3162 [22]

Fig. 1: Linear increase in power consumption with increasing sampling rate in the ADC and the DAC of a USRP. Reproduced from [15]

setup and simulation results. The experimental setup on the ORBIT testbed and corresponding results are presented in Section V and we conclude in Section VI.

II. Related work

While optimizing communication links for total transmit power is a well studied area, in recent years, optimizing a communication link for total power consumption is an active area of research growing in importance. The authors of [23] consider the effect of system power for energy efficient wireless communications. Modulation schemes optimized for system power consumption are studied in [24], while the authors in [25] present a communication-theoretic view of system power consumption. System power constraints specifically related to NC-OFDM are studied in in [26], [27], where it is shown that the maximum spectrum span is limited by the power consumption at the ADCs/DACs [26] and that the requirement of a guardband affects the overall system throughput. The authors in [15] characterize the trade-off between the system power and spectrum span from a cross-layer perspective in a multi-hop network. The authors in [28] provide a graph coloring method for spectrum allocation with the goal of providing equal rates to each user. Earlier works have not considered fair spectrum allocation with system power considerations for an NC-OFDM-enabled system. Our work focuses on opportunistic spectrum allocation to maximize the minimum rate while limiting the spectrum span of the NC-OFDM-enabled cognitive radio links.

III. System Model

We consider a network of N point-to-point links that use NC-OFDM for communication. The set of N links in this model is represented by $\mathcal{N}$. These links have access to M channels, represented by the set $\mathcal{M} = \{1, 2, \ldots, M\}$, with each channel having a bandwidth of W Hz. We assume that each channel consists of t OFDM subcarriers. Transceivers in these links can be dynamically programmed to use different sets of channels. The distance between the transmitter and the receiver in link l is denoted as d_l. We assume that each channel experiences flat fading and the channel gain for link l on the mth channel is represented as g_l^m. The link gain encompasses antenna gain, path-loss, shadowing and fading. The transmit power used by each link l on all channels m is kept at a constant value p throughout this paper. Hence, the received power at the receiver of link l on the channel m is given by pg_l^m. The M available channels are distributed among the N links in a orthogonal manner while ensuring some measure of fairness. The $N \times M$ channel allocation matrix resulting from such a process is denoted by $\mathbf{A}$ Elements of matrix $\mathbf{A}$ can either be 1 or 0. The ith row of $\mathbf{A}$ represents the channel allocation vector for the ith link. Elements of $\mathbf{A}$ are defined as follows

$$a_{lm} = \begin{cases} 1, & \text{link } l \text{ is scheduled on channel } m \in \mathcal{M} \\ 0, & \text{otherwise.} \end{cases}$$

Since we assume that all N links in our model can potentially interfere with each other, we restrict ourselves to disjoint or orthogonal allocation of the available channels. Thus,

$$\sum_{l=1}^{N} a_{lm} \leq 1, \quad \forall\, m \in \mathcal{M}. \tag{1}$$

We also assume that the number of channels M is more than the number of links N and therefore, any fair allocation would not leave any link without any channel.

As discussed in the previous section, the total spectrum span of a cognitive link affects the sampling rate and hence the system power. Fig. 1 reproduced from [15], shows the power consumption in the ADCs and DACs that are typically used in USRP radios as a function of sampling rate. Higher bandwidth usage results in higher sampling rate, and this increases system power consumption in the ADC and DAC.

Therefore, it becomes important to keep the overall spread of frequencies over which the channels are allocated to a link to a reasonably small value. We define the spectrum span B_l for a link l as the magnitude of the difference in the frequencies used by the channels with smallest and largest index. For a link l, spectrum span can be written as

$$B_l = \Big(\max_{m \in \mathcal{M}} (m \cdot a_{lm}) - \min_{m \in \mathcal{M}} (m \cdot a_{lm} + M(1 - a_{lm})) + 1 \Big) \cdot W. \tag{2}$$

We define a threshold b for the spectrum span such that

$$B_l \leq b \cdot W \quad \forall\, l \in \mathcal{N} \tag{3}$$

where $b \leq M$.

We also assume that each of the N links experience interference from a different set of out-of-network interfering nodes and that we have no control over these interfering nodes. The $N \times M$ matrix $\mathbf{U}$ represents the cumulative interference power observed by the links from these out-of-network interferers on each of the M channels. Each element u_{lm} of this matrix represents the total out-of-network interference power observed by the receiver of link l on channel m. In this scenario, the signal-to-interference-plus-noise ratio (SINR) on channel m for the receiver of link l is defined as

$$s_l^m = \frac{p g_l^m}{N_0 W + u_{lm}} \quad \forall\, l \in \mathcal{N},\ m \in \mathcal{M} \tag{4}$$

where N_0 is the noise power spectrum density. Since we have assumed orthogonal channel allocation, we do not consider the interference from other links while calculating the SINR. When the channel m is allocated to link l, the data rate for link l on channel m is given by

$$c_l^m = W \log_2(1 + s_l^m) \quad \forall\, l \in \mathcal{N},\ m \in \mathcal{M}. \tag{5}$$

Depending on whether this channel is allocated to this link or not, the rate r_l^m achieved by link l on this channel satisfies

$$r_l^m = c_l^m a_{lm}. \tag{6}$$

The total data rate achieved by link l is denoted as r_l, and is given by

$$r_l = \sum_{m=1}^{M} r_l^m \quad \forall\, l \in \mathcal{N}. \tag{7}$$

A. Problem formulation

The objective of this paper is to obtain a fair spectrum allocation across all the cognitive links in the system such that (a) it maximizes the minimum data rate among all the links under the condition that the spectrum be allocated in an orthogonal manner and (b) the resulting span is within a specified threshold, so as to limit the overall system power consumption.

To achieve this objective, we formulate an optimization problem to maximize the minimum data rate while restricting the spectrum span to be below a threshold b. Such an optimization problem can be written as follows

TABLE I: List of notations

$\mathcal{N}$	Set of links
N	Number of links
$\mathcal{M}$	Set of total available channels
M	Number of total available channels
$\mathbf{A}$	Resource allocation matrix of size $N \times M$
a_{lm}	Allocation indicator variable for link l and channel m
$\mathbf{U}$	Interference matrix of size $N \times M$
u_{lm}	Interference for link l on channel m
g_l^m	Channel gain for link l using channel m
s_l^m	Signal-to-noise ratio for link l using channel m
c_l^m	Channel capacity for link l using channel m
r_l^m	Data rate for link l using channel m
r_l	Total data rate for link l
d_l	Distance between transmitter and receiver for link l
W	Bandwidth of each channel
N_0	Noise spectrum density

$$\begin{aligned}
&\text{maximize} \quad \min_{l \in \mathcal{N}} r_l \\
&\text{subject to :} \\
&B_l \leq b \cdot W && \forall\, l \in \mathcal{N}, \\
&r_l^m = c_l^m . a_{lm} && \forall\, l \in \mathcal{N},\ \forall\, m \in \mathcal{M}, \\
&r_l = \sum_{m=1}^{M} r_l^m && \forall\, l \in \mathcal{N}, \\
&\sum_{l=1}^{N} a_{lm} \leq 1, && \forall\, m \in \mathcal{M}, \\
&a_{lm} \in \{0, 1\} && \forall\, l \in \mathcal{N},\ \forall\, m \in \mathcal{M}.
\end{aligned}$$

Note that only variables in above formulation are the integer variable a_{lm}, since all the other variables can be eliminated in a straightforward manner. Such a formulation is seen to be an integer linear program. Maximizing the minimum rate and restricting the spectrum span are two competing objectives. Allowing a higher value of b provides the opportunity to allocate the channels over a wider range of possibilities which might result in higher data rate, but this increases the system power consumption. On the other hand keeping the spectrum span threshold too small eliminates these allocation opportunities. We analyze this trade-off in the next section.

In our analysis we do not consider protecting interfering nodes from transmission from any of the links. However, if the interfering nodes are primary users then they can be protected by forcing variable u_{lm} to a large value for channels used by primary users (PUs), thus reducing the channel capacity in the optimization problem to near-zero value for concerned channels. In such a scenario our optimization problem would still hold as long as number of useful channels (channels not used by PUs) is more than the number of point-to-point links in the network.

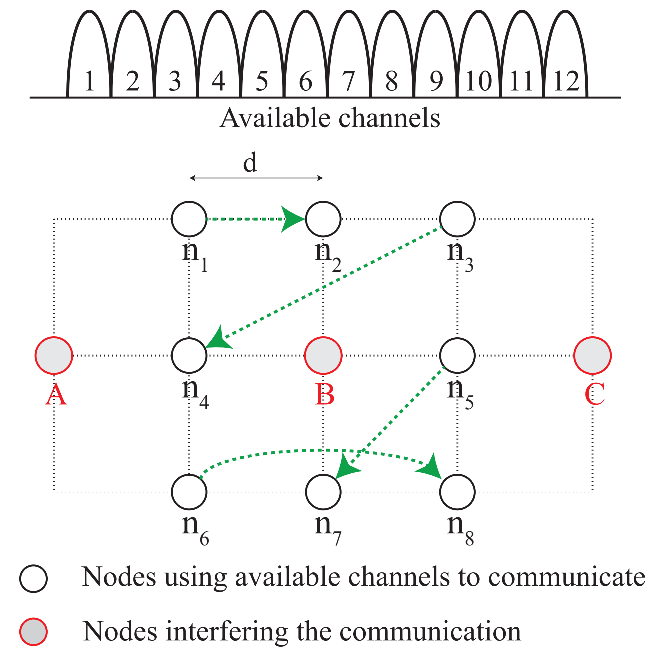

Fig. 2: Available channels and network topology used in the simulation.

Link	Nodes	Length
L_1	$n_1 \to n_2$	d
L_2	$n_3 \to n_4$	$\sqrt{5}d$
L_3	$n_5 \to n_7$	$\sqrt{2}d$
L_4	$n_6 \to n_8$	$2d$

TABLE II: Links in the network used for the simulation.

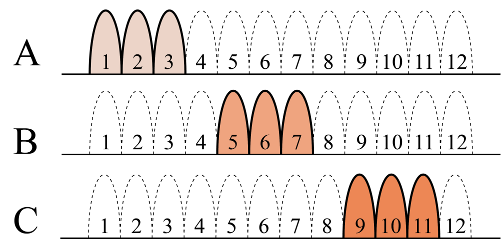

Fig. 3: Channel used by interfering nodes A, B and C.

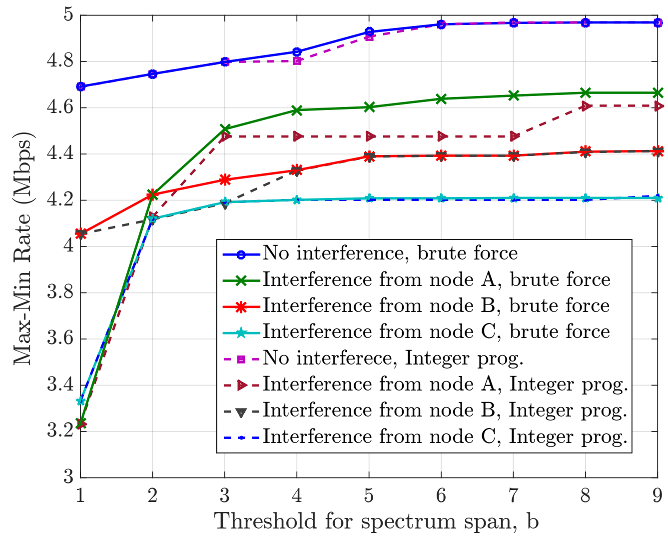

Fig. 4: Max-min rate obtained for varying b in presence of A, B or C.

IV. SIMULATION SETUP

The integer linear program formulated in the previous section can be solved using the MOSEK solver via CVX in MATLAB [29]–[31]. MOSEK solves the integer program using the branch-and-bound method, which is known to have an exponential complexity. Since integer programming is an NP-hard problem, MOSEK uses continuous relaxation with a goal of computing near-optimal solution instead of finding an optimal solution. The output of such an optimization generates a list of channel allocations for each link along with the rates achieved in each of them.

To analyze the effectiveness of the proposed approach, we test it on the topology shown in Fig. 2. As shown in Fig. 2, the nodes named n_1 to n_8 use the available channels in an adaptive manner in the presence of interfering transmitters A, B and C. Nodes n_1, n_3, n_5 and n_6 are assumed to be transmitters, transmitting to nodes n_2, n_4, n_7 and n_8 respectively as shown in table II. In our simulation, we assume that grid spacing is $d = 1$m and that there are 12 channels available for communication, with each channel having a bandwidth of 100 KHz. The transmission power is 0.1mW. The noise power is calculated from the thermal noise power density assuming that our system operates at a temperature of $T = 300$K. For such a system, the parameters corresponding to the system model are given as follows:

$$\mathcal{N} = \{L_1, L_2, L_3, L_4\},$$
$$\mathcal{M} = \{1, 2, 3, 4, 5, 6, 7, 8, 9, 10, 11, 12\},$$
$$W = 100\text{KHz},$$
$$N_0 = kT,$$

where k is the Boltzmann constant.

The channel gain in each of the channels is generated using a Rician flat fading model with K-factor of 30dB. As shown in Fig. 3, interfering nodes A, B and C operate in channels $(1, 2, 3)$, $(5, 6, 7)$ and $(9, 10, 11)$ respectively. These interfering nodes are transmitting at 33dB higher power than the noise power. We assume that these interfering nodes can be turned on or off independent of each other.

As mentioned in the previous section, there exists a trade-off between the max-min rate and the restriction on the spectrum span. Clearly, the highest value of the max-min rate can be achieved when $b = M$. Obtaining this trade-off curve requires us to compute the globally optimal max-min rate for every value of b. Since integer programming is an NP-Hard problem, computing the globally optimal solution is not possible using solvers such as MOSEK and must instead be computed in a brute-force manner by considering all possible channel allocations. A trade-off curve obtained through a brute-force search is shown in Fig. 4. Specifically, Fig. 4

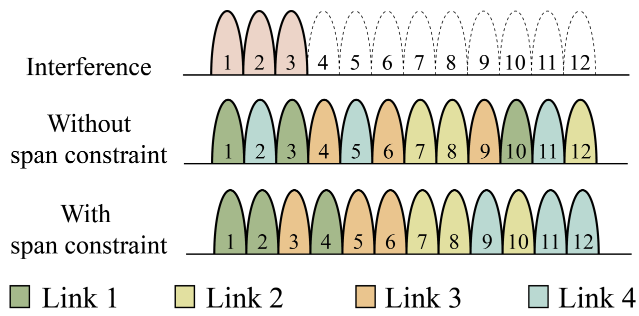

Fig. 5: Channel allocation for the links in presence of interference from node 'A', with and without span constraint of $b = 4$.

plots the trade-off curve between the max-min rate and the spectrum span for four scenarios where the four in-network links see interference from either (i) node A only, (ii) node B only, (iii) node C only or (iv) see no interference at all. Fig. 4 also plots the max-min rate obtained by solving the integer program presented in Section III-A. Although solving the integer program is not guaranteed to find the globally optimal solution, it is seen that the overall average performance is relatively close to that obtained from a brute-force search. This highlights the effectiveness of the proposed framework.

Fig. 4 also shows that the max-min rate saturates well before the restriction on the spectrum span is increased to M. This indicates that the threshold b that limits the spectrum span can be set to a value significantly lesser than M while paying only a small penalty in the max-min rate.

Fig. 5 illustrates the effect of the span constraint on the channel allocation for a particular instance of the channel gains and when only node A causes interference. It is seen that channel allocation without any restriction on span can result in a link being allocated channels across a wide spectrum. However, with a span constraint of $b = 4$, spectrum gets reallocated so as to satisfy the span constraint while not incurring a significant penalty on the max-min rate.

Fig. 6 shows the change in throughput for each of the four links before and after the introduction of interference from node A. The spectrum span is restricted to be less than or equal to 4. The figure plots the throughput obtained when (a) spectrum is optimally allocated when there is no interference, (b) interference from node A is introduced, but spectrum allocation remains the same as in case (a), and (c) spectrum is reallocated while accounting for the interference from node A. As expected throughput drops from case (a) to case (b) but then increases after reallocation in case (c). While the frequency of spectrum reallocation is certainly a function of the changes in the interference landscape, how often such a reallocation is permissible or necessary is also dependent on other application specific constraints and hardware limitations and is beyond the scope of this paper.

V. Experiments on ORBIT testbed

A. Platform

We test the proposed formulation on a scaled-down version of the network (see Fig. 2) used for simulations in Section IV.

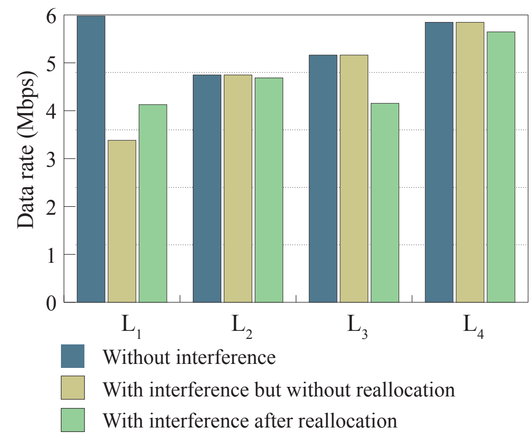

Fig. 6: Data rate obtained by solving optimization problem with and without interference from node 'A', $b = 4$.

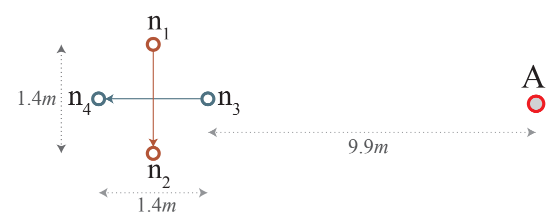

Fig. 7: Topology used in the ORBIT testbed.

For the experimental setup we consider a network consisting of two links along with one out-of-network interferer, as shown in Fig. 7. The two point-to-point links are denoted as $L_1 = (n_1, n_2)$ and $L_2 = (n_3, n_4)$, and the interfering node is labeled as node A. Each node is a USRP2 node running on the GNU Radio software platform. These nodes are part of the larger ORBIT testbed that consists of 400 radio nodes placed in a 20×20 grid with $1m$ spacing between the adjacent nodes. The testbed nodes are equipped with a variety of radio platforms including 802.11 a/b/g, Bluetooth, Zigbee, and various versions of software defined radios (SDRs) such as USRP platforms, WARP platforms, and the CRKit cognitive radios that was developed at WINLAB [16], [32], [33]. The nodes in our experiments are USRP N210 modules with SBX transceiver daughter-card that can operate anywhere from 400 MHz to 4.4 GHz and transmit up to 100 mW of power. GNU Radio is a free and open-source SDR framework that provides the application programming interface (API) for several hardware platforms, including many USRP devices. The NC-OFDM communication paths are implemented in C++ and Python in GNU Radio. Fig. 8 represents the block diagram of the transmitter and receiver in our experimental setup.

B. Experiment

The experiment is designed to allow for simultaneous operation of the two links. Both the links have access to a total bandwidth of 1 MHz and transmit using a carrier frequency of 1.5 GHz. The 1 MHz bandwidth is divided into 128 subcarriers. The size of a data packet is set to 1500 bytes. Among the available 128 subcarriers, only 112 subcarriers are used for data transmission. The remaining 16 subcarriers are used for

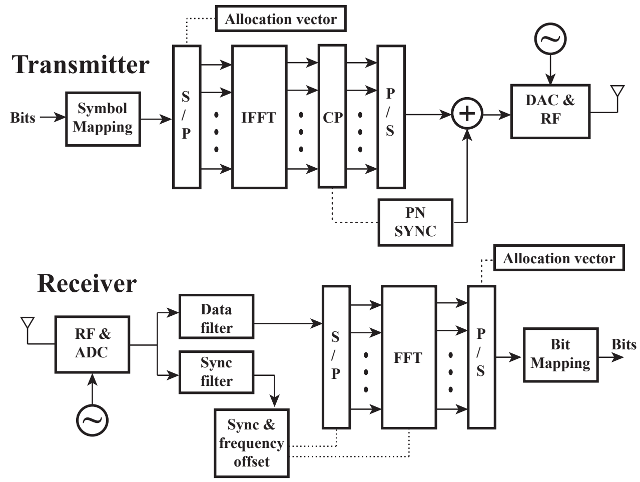

Fig. 8: Block diagram for implementation of NC-OFDM with GNU Radio.

Input: **A**, r_l^m, r_l
Output: **A**
l_b = link using channel 1
m_b = 1
for $m = 2$ to M **do**
  l_n = link using channel m
  if (($l_n \neq l_b$) and ($l_n \neq$ NULL)) **then**
    if $((r_{l_n} - r_{l_n}^m) \leq (r_{l_b} - r_{l_b}^{m_b}))$ **then**
      $a_{l_n m} = 0,$
      $r_{l_n}^m = 0,$
    else
      $a_{l_b m_b} = 0,$
      $r_{l_b}^{m_b} = 0,$
    end if
  end if
  m_b = m
  l_b = l_n
end for
return A

Fig. 9: Pseudocode for creating guardband after channel allocation using proposed method.

control and synchronization purposes. Our experiments on this setup revealed that OFDM implementations using the USRP2 platform are not robust when using less than 4 subcarriers on a single link. Hence, we group the 112 data subcarriers into groups of 4 subcarriers each to form 28 channels, each of bandwidth 31.25 KHz.

A significant challenge that affected synchronization as well as data transmission while running our experiment was interference from the sidelobes of adjacent channels that were being used by either the interferer or the other link in the network. Different methods of handling the issue of sidelobe power have been proposed including the usage of a guardband or techniques for sidelobe suppression [34]–[36]. While this problem can also be addressed by designing filters with sharp cut-offs, such a solution is not practical in a dynamic system where spectrum allocation changes constantly. To resolve issues with synchronization due to sidelobe interference, we set aside 8 subcarriers at either ends of the 1 MHz spectrum exclusively for synchronization in each of the two links. For each link, robust synchronization was achieved by transmitting PN-sequence preambles [37] through the 8 dedicated subcarriers assigned to that link. To address sidelobe interference among the data subcarriers, subsequent to channel allocation by the integer program, a guardband is introduced whenever adjacent subcarriers are assigned to different links. The guardband is created by nulling one of the two adjacent channels, resulting in a small loss in throughput while increasing the overall signal quality. The pseudocode for deciding which of the two adjacent channels to null is presented in Fig. 9, and operates on the principle of nulling the channel that leads to the smallest drop in throughput. Fig. 8 presents a block diagram of our implementation of NC-OFDM using GNU Radio; note the separation between the data and synchronization paths at the receiver.

Due to the short distance between the USRP nodes in the experimental setup, the channel gains between the nodes is approximated using a line-of-sight path loss model. Channel allocation was carried out at a centralized location using the framework proposed in Section III-A. The allocated channels were then conveyed to each of the two links, which was followed by the insertion of guardbands as described earlier.

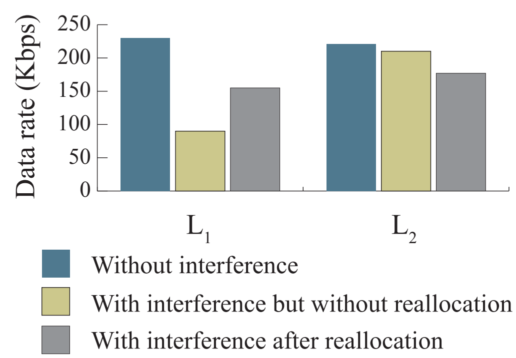

Fig. 10: Data rate obtained in the ORBIT testbed.

Fig. 10 plots the throughput achieved in each of the two links through such an experimental setup. The results in Fig. 10 are follow the same general trend that was observed in Fig. 6 despite the insertion of guardbands and the lack of perfect channel knowledge.

VI. Conclusion

This paper considered the problem of fair spectrum allocation in NC-OFDM-enabled point-to-point links in the presence of interfering nodes while imposing a spectrum span constraint. Assuming a fixed transmit power across all subcarriers and orthogonal spectrum allocation, we formulated an integer linear program to maximize the minimum rate in the network under certain spectrum span constraints. Such an optimization problem can be efficiently solved using readily available solvers. It was seen that there exists a clear trade-off between the spectrum span and the max-min rate. Simulation results indicated that the spectrum span can be restricted to a relatively small number without adversely affecting the overall throughput of the system. An experimental evaluation of the techniques developed in this paper using USRP enabled ORBIT radio network testbed was also presented. Experimental results further strengthen the general trend observed in simulations.

ACKNOWLEDGMENT

This work is supported in part by a grant from the U.S. Office of Naval Research (ONR) under grant number N00014-15-1-2168.

REFERENCES

[1] J. Mitola and G. Q. Maguire Jr., "Cognitive radio: making software radios more personal," *IEEE Trans. Prof. Commun.*, vol. 6, no. 4, pp. 13–18, Aug. 1999.

[2] E. Biglieri, A. J. Goldsmith, L. J. Greenstein, N. B. Mandayam, and H. V. Poor, *Principles of cognitive radio*. Cambridge University Press, 2012.

[3] S. Haykin, "Cognitive radio: brain-empowered wireless communications," *IEEE J. Sel. Areas Commun.*, vol. 23, no. 2, pp. 201–220, Feb. 2005.

[4] R. Thomas, L. DaSilva, and A. MacKenzie, "Cognitive networks," in *Proc. IEEE Symp. on New Frontiers in Dynamic Spectrum Access Networks (DySPAN)*, Nov. 2005, pp. 352–360.

[5] O. Ileri and N. B. Mandayam, "Dynamic spectrum access models: toward an engineering perspective in the spectrum debate," *IEEE Commun. Mag.*, vol. 46, no. 1, pp. 153–160, Jan. 2008.

[6] Y.-C. Liang, Y. Zeng, E. Peh, and A. T. Hoang, "Sensing-throughput tradeoff for cognitive radio networks," *IEEE Trans. Wireless Commun.*, vol. 7, no. 4, pp. 1326–1337, Apr. 2008.

[7] S. Srinivasa and S. A. Jafar, "Cognitive radios for dynamic spectrum access - The throughput potential of cognitive radio: A theoretical perspective," *IEEE Commun. Mag.*, vol. 45, no. 5, pp. 73–79, May 2007.

[8] M. Cesana, F. Cuomo, and E. Ekici, "Routing in cognitive radio networks: challenges and solutions," *Ad Hoc Netw.*, vol. 9, no. 3, pp. 228–248, May 2011.

[9] G. Cheng, W. Liu, Y. Li, and W. Cheng, "Joint on-demand routing and spectrum assignment in cognitive radio networks," in *Proc. IEEE Int. Commun. Conf. (ICC)*, Jun. 2007, pp. 6499–6503.

[10] M. N. Islam, N. Mandayam, and S. Kompella, "Optimal resource allocation and relay selection in bandwidth exchange based cooperative forwarding," in *Proc. IEEE Int. Symp. on Modeling and Optimization in Mobile, Ad Hoc and Wireless Netw. (WiOpt)*, 2012, pp. 192–199.

[11] T. A. Weiss and F. K. Jondral, "Spectrum pooling: an innovative strategy for the enhancement of spectrum efficiency," *IEEE Commun. Mag.*, vol. 42, no. 3, pp. S8–S14, Mar. 2004.

[12] R. Rajbanshi, A. M. Wyglinski, and G. J. Minden, "An efficient implementation of NC-OFDM transceivers for cognitive radios," in *Proc. EAI Int. Conf. on Cognitive Radio Oriented Wireless Netw. and Commun. (CROWNCOM)*, Jun. 2006.

[13] L. Yang, Z. Zhang, W. Hou, B. Y. Zhao, and H. Zheng, "Papyrus: A software platform for distributed dynamic spectrum sharing using SDRs," *ACM SIGCOMM Comput. Commun. Review*, vol. 41, pp. 31–37, 2011.

[14] L. Yang, B. Y. Zhao, and H. Zheng, "The spaces between us: Setting and maintaining boundaries in wireless spectrum access," in *Proc. ACM Annual Int. Conf. on Mobile Computing and Netw. (MobiCom)*, Sep. 2010, pp. 37–48.

[15] M. N. Islam, N. B. Mandayam, S. Kompella, and I. Seskar, "Power optimal non-contigous spectrum access," submitted for publication in *IEEE Trans. Wireless Commun.*, 2013. [Online]. Available: http://arxiv.org/abs/1309.0861

[16] USRP software radio systems: Ettus Resarch. [Online]. Available: http://www.ettus.com/

[17] D. Raychaudhuri, N. B. Mandayam, J. B. Evans, B. J. Ewy, S. Seshan, and P. Steenkiste, "CogNet: An architectural foundation for experimental cognitive radio networks within the future internet," in *Proc. Int. Workshop on Mobility in the Evolving Internet Architecture (MobiArch)*, Dec. 2006, pp. 11–16.

[18] GNU Radio Website, accessed February 2012. [Online]. Available: http://www.gnuradio.org

[19] Texas Instruments, Inc., "Datasheet for ADS62P4X: Dual channel, 14 bits, 125/105/80/65 MSPS ADC with DDR LVDS/CMOS outputs." [Online]. Available: http://www.ti.com/lit/ds/symlink/ads62p42.pdf

[20] ——, "Datasheet for ADS4249: Dual-Channel, 14-Bit, 250-MSPS Ultralow-Power ADC." [Online]. Available: http://www.ti.com/lit/ds/symlink/ads4249.pdf

[21] Analog Devices, Inc., "Datasheet for AD9777: 16-bit interpolating dual DAC converter." [Online]. Available: http://www.analog.com/media/en/technical-documentation/data-sheets/AD9777.pdf

[22] Texas Instruments, Inc., "Datasheet for DAC3152/DAC3162: Dual-Channel, 10-/12-Bit, 500-MSPS Digital-to-Analog Converters." [Online]. Available: http://www.ti.com/lit/ds/symlink/dac3162.pdf

[23] G. Li, Z. Xu, C. Xiong, C. Yang, S. Zhang, Y. Chen, and S. Xu, "Energy-efficient wireless communications: tutorial, survey, and open issues," *IEEE Trans. Wireless Commun.*, vol. 18, no. 6, pp. 28–35, Dec. 2011.

[24] S. Cui, A. Goldsmith, and A. Bahai, "Energy-constrained modulation optimization," *IEEE Trans. Wireless Commun.*, vol. 4, no. 5, pp. 2349–2360, Sep. 2005.

[25] P. Grover, K. Woyach, and A. Sahai, "Towards a communication-theoretic understanding of system-level power consumption," *IEEE J. Sel. Areas Commun.*, vol. 29, no. 8, pp. 1744–1755, Sep. 2011.

[26] J. Jia and W. Zhuang, "Capacity of multi-hop wireless network with frequency agile software defined radio," in *Proc IEEE Int. Conf. Comput. Commun. (INFOCOM)*, Apr. 2011, pp. 41–46.

[27] L. Cao, L. Yang, and H. Zheng, "The impact of frequency-agility on dynamic spectrum sharing," in *Proc. IEEE Symp. on New Frontiers in Dynamic Spectrum Access Networks (DySPAN)*, Apr. 2010.

[28] G. Zhang and S. Feng, "Subcarrier allocation algorithms based on graph-coloring in cognitive radio NC-OFDM system," in *IEEE Int. Conf. Comput. Science and Information Technol. (ICCSIT)*, July 2010, pp. 535–540.

[29] CVX Research, Inc., "CVX: Matlab software for disciplined convex programming, version 2.0 beta," Sep. 2012. [Online]. Available: http://cvxr.com/cvx

[30] M. Grant and S. Boyd, "Graph implementations for nonsmooth convex programs," in *Recent Advances in Learning and Control*, ser. Lecture Notes in Control and Information Sciences, V. Blondel, S. Boyd, and H. Kimura, Eds. Springer-Verlag Limited, 2008, pp. 95–110.

[31] MOSEK ApS, *The MOSEK optimization toolbox for MATLAB manual. Version 7.1 (Revision 28).*, 2015. [Online]. Available: http://docs.mosek.com/7.1/toolbox/index.html

[32] WINLAB, Rutgers, The State University of New Jersey. ORBIT: Open access research testbed for next-generation wireless networks. [Online]. Available: http://www.orbit-lab.org

[33] P. Murphy, A. Sabharwal, and B. Aazhang, "Design of WARP: A wireless open-access research platform," in *European Signal Process. Conf. (EUSIPCO)*, Sep. 2006.

[34] D. Li, X. Dai, and H. Zhang, "Sidelobe suppression in NC-OFDM systems using constellation adjustment," *IEEE Commun. Lett.*, vol. 13, no. 5, pp. 327–329, May 2009.

[35] A. Ghassemi, L. Lampe, A. Attar, and T. Gulliver, "Joint sidelobe and peak power reduction in OFDM-based cognitive radio," in *IEEE Veh. Technol. Conf. (Fall)*, Sep. 2010.

[36] Z. Yuan and A. M. Wyglinski, "On sidelobe suppression for multicarrier-based transmission in dynamic spectrum access networks," *IEEE Trans. Veh. Technol.*, vol. 59, no. 4, pp. 1998–2006, May 2010.

[37] F. Tufvesson, O. Edfors, and M. Faulkner, "Time and frequency synchronization for OFDM using PN-sequence preambles," in *IEEE Veh. Technol. Conf. (Fall)*, Sep. 1999, pp. 2203–2207.